Acta Crystallographica Section B
Structural Science
ISSN 0108-7681

Atomic displacements at and order of all phase transitions in multiferroic $YMnO_3$ and $BaTiO_3$

S. C. Abrahams

Physics Department, Southern Oregon University, Ashland, OR 97520, USA

Correspondence e-mail: sca@mind.net

Received 4 April 2009
Accepted 3 June 2009

Coordinate analysis of the multiple phase transitions in hexagonal $YMnO_3$ leads to the prediction of a previously unknown aristotype phase, with the resulting phase-transition sequence: $P6_3'cm'$(*e.g.*) $\leftrightarrow$ $P6_3cm$ $\leftrightarrow$ $P6_3/mcm$ $\leftrightarrow$ $P6_3/mmc$ $\leftrightarrow$ $P6/mmm$. Below the Néel temperature $T_N \simeq 75$ K, the structure is antiferromagnetic with the magnetic symmetry not yet determined. Above T_N the $P6_3cm$ phase is ferroelectric with Curie temperature $T_C \simeq 1105$ K. The nonpolar paramagnetic phase stable between T_C and ~ 1360 K transforms to a second nonpolar paramagnetic phase stable to ~ 1600 K, with unit-cell volume one-third that below 1360 K. The predicted aristotype phase at the highest temperature is nonpolar and paramagnetic, with unit-cell volume reduced by a further factor of 2. Coordinate analysis of the three well known phase transitions undergone by tetragonal $BaTiO_3$, with space-group sequence $R3m$ $\leftrightarrow$ $Amm2$ $\leftrightarrow$ $P4mm$ $\leftrightarrow$ $Pm\bar{3}m$, provides a basis for deriving the aristotype phase in $YMnO_3$. Landau theory allows the I $\leftrightarrow$ II, III $\leftrightarrow$ IV and IV $\leftrightarrow$ V phase transitions in $YMnO_3$, and also the I $\leftrightarrow$ II phase transition in $BaTiO_3$, to be continuous; all four, however, unambiguously exhibit first-order characteristics. The origin of phase transitions, permitted by theory to be second order, that are first order instead have not yet been thoroughly investigated; several possibilities are briefly considered.

1. Introduction

Interest in the multiferroic properties of hexagonal $YMnO_3$ and family,[1] with both the number and temperatures of phase transitions being controversial, has recently increased sharply. Huang *et al.* (1997) detected anomalies, indicative of coupling between ferroelectric and antiferromagnetic ordering, in the dielectric constant of $YMnO_3$ near its magnetic Néel temperature $T_N \simeq 80$ K. Janoschek *et al.* (2005) reported the slightly pressure-dependent magnetic moment of $YMnO_3$ as 3.09 (2) μ_B at 1.5 K, decreasing smoothly with T to zero at $T_N \simeq 80$ K. Fujimura *et al.* (2007) detected anomalies in the relative dielectric permittivity accompanying the antiferromagnetic transition near T_N at ~ 76 K, while Lancaster *et al.* (2007) reported two oscillatory relaxing signals due to magnetic order below $T_N \simeq 70$ K that increase, under the application of hydrostatic pressure, as the ordered moment decreases. Lee *et al.* (2008) reported a structural transition at $T_N \simeq 75$ K, characterized by changes of ~ 0.05–0.09 Å in atomic location, ~ 0.05 A mol^{-1} in magnetic susceptibility and ~ 13 J mol^{-1} K^{-1} in entropy.

[1] The dielectric and magnetic properties of metastable orthorhombic $YMnO_3$ (space group *Pnma*), with $T_C \simeq 30$ K and $T_N \simeq 40$ K, are also of current interest but are not considered further here.

Table 1
Ambient atomic coordinates of $YMnO_3$ in phase IV (Aken *et al.*, 2001) and hypothetical $x'y'z'$ coordinates for intermediate phase III with supergroup $P6_3/mcm$ symmetry, with Δx, Δy, Δz and ambient lattice constants.

Thermal/static u_{33} displacements in Å. a = 6.1387 (3), c = 11.4071 (9) Å, with polar $z_{IV} = z^*_{IV} + \frac{1}{4}$ and $z'_{IV} = z_{IV} + 0.00246$, where z^*_{IV} is a z-coordinate value of van Aken *et al.* (2001).

	Wyckoff position									Δx_{IV-III}†	Δy_{IV-III}	Δz_{IV-III}	$\Delta\xi_{IV-III}$	
	$P6_3cm$‡	$P6_3/mcm$	x_{IV}	y_{IV}	z_{IV}	z'_{IV}	x_{III}	y_{III}	z_{III}	(Å)	(Å)	(Å)	(Å)	u_{33}§
Phase IV → III														
Y1	2*a*	2*b*	0	0	0.52122 (12)	0.52368	0	0	$\frac{1}{2}$	0	0	0.270	0.270	0.09
Y2	4*b*	4*d*	$\frac{1}{3}$	$\frac{2}{3}$	0.48041 (3)	0.48287	$\frac{1}{3}$	$\frac{2}{3}$	$\frac{1}{2}$	0	0	−0.195	0.195	0.12
Mn	6*c*	6*g*	0.3352 (4)	0	0.24688 (12)	0.24934	0.3352	0	$\frac{1}{4}$	0	0	−0.008	0.008	0.08
O1	6*c*		0.3083 (12)	0	0.4096 (7)	0.4121	0.3335	0	0.4127	−0.155	0	−0.007	0.155	0.12
		12*k*												
O2	6*c*		0.3587 (10)	0	0.0841 (6)	0.0866	0.3335	0	0.087	0.155	0	−0.008	0.155	0.14
O3	2*a*	2*a*	0	0	0.2251 (12)	0.2276	0	0	$\frac{1}{4}$	0	0	−0.256	0.256	0.12
O4	4*b*	4*c*	$\frac{1}{3}$	$\frac{2}{3}$	0.2655 (11)	0.2680	$\frac{1}{3}$	$\frac{2}{3}$	$\frac{1}{4}$	0	0	0.205	0.205	0.07

† $\Delta x = (x - x') \cdot a$, $\Delta y = (y - y') \cdot a$ and $\Delta z = (z - z') \cdot c$, with $\Delta\xi_i = [(x_i - x'_i)^2 + (y_i - y'_i)^2 + (x_i - x'_i)(y_i - y'_i) + (z_i - z'_i)^2]^{1/2}$. ‡ Wyckoff positions in $P6_3cm$: 2*a* 0,0,*z*; 0,0,*z* + $\frac{1}{2}$; 4*b* $\frac{1}{3},\frac{2}{3},z$; $\frac{2}{3},\frac{1}{3},z+\frac{1}{2}$; $\frac{2}{3},\frac{1}{3},z$; $\frac{1}{3},\frac{2}{3},z+\frac{1}{2}$; 6*c* *x*,0,*z*; 0,*x*,*z*; $\bar{x},\bar{x},z$; $\bar{x},0,\frac{1}{2}+z$; $0,\bar{x},\frac{1}{2}+z$; *x*,*x*,$\frac{1}{2}+z$. In $P6_3/mcm$: 2*a* 0,0,$\frac{1}{4}$; 0,0,$\frac{3}{4}$; 2*b* 0,0,0; 0,0,$\frac{1}{2}$; 4*c* $\frac{1}{3},\frac{2}{3},\frac{1}{4}$; $\frac{2}{3},\frac{1}{3},\frac{3}{4}$; $\frac{2}{3},\frac{1}{3},\frac{1}{4}$; $\frac{1}{3},\frac{2}{3},\frac{3}{4}$; 4*d* $\frac{1}{3},\frac{2}{3},0$; $\frac{1}{3},\frac{2}{3},\frac{1}{2}$; $\frac{2}{3},\frac{1}{3},0$; $\frac{2}{3},\frac{1}{3},\frac{1}{2}$; 6*f* $\frac{1}{2},0,0$; $0,\frac{1}{2},0$; $\frac{1}{2},0,\frac{1}{2}$; $0,\frac{1}{2},\frac{1}{2}$; $\frac{1}{2},\frac{1}{2},0$; $\frac{1}{2},\frac{1}{2},\frac{1}{2}$; 12*k* ±(*x*,0,*z*; 0,*x*,*z*; $\bar{x},\bar{x},z$; $\bar{x},0,\frac{1}{2}+z$; $0,\bar{x},\frac{1}{2}+z$; *x*,*x*,$\frac{1}{2}+z$). § Thermal and/or static atomic amplitudes u_{33} in Å for Y and In, u_{eq} for O, at ambient T.

Group-theoretical analysis by Lonkai *et al.* (2004), combined with X-ray and neutron powder diffraction determinations of the isomorphous structures RMnO$_3$ for R = Yb, Lu and Tm over the range 300–1400 K, confirmed the suggestive but previously nondefinitive anomalies at ∼ 935 K apparent in Ismailzade & Kizhaev's (1965) unit-cell lengths for $YMnO_3$ between 0 and 1075 K. Similar indications of a $YMnO_3$ phase transition at ∼ 925 K are also present in Łukaszewicz & Karut-Kalicińska's (1974) data; the latter unambiguously identified a still higher temperature phase transition at ∼ 1275 K in which a unit cell forms with a volume one-third that at ambient temperature and determined the structure therein. Lonkai *et al.* (2004) interpreted the $YMnO_3$ transition at 1050 (50) K as from ferroelectric $P6_3cm$ to a mode with P_S = 0, but without a change in the space group, followed by a transition to nonpolar $P6_3/mmc$ at T_{NP} = 1433 (27) K with unit-cell volume above T_{NP} one-third that below. Assuming the order parameter causes small changes in the experimental diffraction pattern, they concluded that $YMnO_3$ and isomorphous family members are improper ferroelectrics.

Kim *et al.* (2000) determined the spontaneous polarization of single-crystal $YMnO_3$ at ambient temperature over a wide frequency range to be $P_S = 4.5 \times 10^{-2}$ C m^{-2}, with a coercive field of 190 V m^{-1}. Katsufuji *et al.* (2002) reported that the lattice constants and resistivity of RMnO$_3$ (R = Y, Lu, Sc) vary continuously between 300 and 1000 K and suggested that T_C is likely to exceed 1000 K; they noted that magnetic diffuse neutron scattering in $LuMnO_3$ remains detectable as high as $\sim 3T_N$, *i.e.* $\gtrsim$ 220 K.

van Aken *et al.* (2004) proposed a two space-group model for $YMnO_3$ on the basis of cooperative 'long-range dipole–dipole interactions and oxygen rotations', as did Jeong *et al.* (2007) who detected only one high-temperature phase transition at ∼ 1250 K below the upper limit of 1400 K in their neutron powder diffraction study. Fennie & Rabe's (2008) group-theoretical analysis and first-principles density-functional calculations for $YMnO_3$ led them also to suggest that the phase transition at ∼ 1270 K is improper, supporting Lonkai *et al.*'s (2004) model.

Subsequent differential thermal analysis by Nénert *et al.* (2005, 2006, 2007) detected two high-temperature phase transitions in $YMnO_3$, at ∼ 1105 and ∼ 1365 K, confirming both by single-crystal dilatometry in a synchrotron X-ray powder investigation between ambience and 1475 K. They determined $YMnO_3$ to be a proper, rather than an improper, ferroelectric and presented additional experimental and theoretical evidence for the formation of an intermediate paraelectric phase with space group $P6_3/mcm$ between the polar and highest known temperature phases.

The frequency at which new studies concerning the multiferroic properties of $YMnO_3$ have appeared, together with several previous controversial assignments of symmetry and increasing interest in phase-transition order, led to the present study in which coordinate analysis for $YMnO_3$ establishes the full phase-transition sequence, based in part on the analysis of the multiphase transitions in multiferroic $BaTiO_3$.

2. Phases of multiferroic hexagonal $YMnO_3$

2.1. Hexagonal $YMnO_3$ phase-transition temperatures

Hexagonal $YMnO_3$ clearly exhibits no less than four rather than the two phases previously recognized, as noted in §1. A new fifth aristotype phase, with space group $P6/mmm$ and no variable z parameter, is predicted herein to form at $T \gtrsim$ 1600 K, see §3.3. The IUCr nomenclature presented previously, on the basis of Tolédano *et al.*'s (1998) recommendations, for the two $YMnO_3$ phases then known (Abrahams, 2001) consequently requires revision as follows:

I | 1600 K | $P6/mmm$ (191) | Z = 1| nonpolar, paramagnetic | phase I unit-cell volume ≃ 1/6 that of phases III, IV or V | predicted zero-parameter structure.

II | ∼ 1360 – $\gtrsim$ 1600 K | $P6_3/mmc$ (194)| Z = 2| nonpolar, paramagnetic | unit-cell volume ≃ 1/3 that of phases III, IV or V.

Table 2
Atomic coordinates of $YMnO_3$ in phase IV (Aken *et al.*, 2001), transformed to the orientation of phase II.

Hypothetical coordinates for phase II in supergroup $P6_3/mmc$ and corresponding Δx, Δy, Δz differences between structures of phases IV and II together with original thermal/static u_{33} displacements in Å. Lattice constants for a_{III} transformed as below. The unit-cell volume in phase II is one-third that of phase IV (Łukaszewicz & Karut-Kalicińska, 1974). Ambient temperature a_{II} axis equivalent at is $a_{IV}/(3)^{1/2} \simeq 3.54$ Å with $c_{II} \simeq c_{IV} \simeq 11.40$ Å; $z'_{II} = z_{II} + \frac{1}{4}$; $z^*_{IV} = z'_{IV} + 0.00246$.

	Wyckoff position											
	$P6_3cm$†	$P6_3/mmc$‡	x_{IV}	y_{IV}	z_{IV}	z'_{IV}	x_{II}	y_{II}	z_{II}	Δx_{IV-II} (Å)	Δy_{IV-II} (Å)	Δz_{IV-II} (Å)	$\Delta\xi_{IV-II}$ (Å)
Phase IV → II													
Y1	1*a*		0.0	0.0	0.52122 (12)	0.52368	0	0	$\frac{1}{2}$	0	0	0.270	0.270
		2*a*											
Y2	1*a*		0.0	0.0	0.98041 (3)	0.98287	0	0	0	0	0	−0.195	0.195
Mn	2*b*	2*d*	0.6704	0.3352 (4)	0.24688 (1)	0.24934	$\frac{2}{3}$	$\frac{1}{3}$	$\frac{1}{4}$	0.013	0.007	−0.008	0.019
O1	2*b*		0.6166	0.3083 (12)	0.4096 (7)	0.4121	$\frac{2}{3}$	$\frac{1}{3}$	0.412	−0.177	−0.089	−0.008	0.235
		4*f*											
O2	2*b*		0.7174	0.3587 (10)	0.0841 (6)	0.0866	$\frac{2}{3}$	$\frac{1}{3}$	0.087	0.179	0.090	−0.007	0.237
O3	1*c*		0.0	0.0	0.2251 (12)	0.2276	0	0	$\frac{1}{4}$	0	0	−0.256	0.256
		2*b*											
O4	1*c*		0.0	0.0	0.7655 (11)	0.7680	0	0	$\frac{3}{4}$	0	0	0.205	0.205

† Atomic coordinates and Wyckoff positions in Table 2 were modified for unit-cell volume reduction by a factor of 3 and reorientated to match the phase I structure. The insignificant difference between experimental Mn(x) and Mn(y) magnitudes, and at the special position $\frac{2}{3}, \frac{1}{3}$, is noted. ‡ Wyckoff positions in $P6_3/mmc$: 2*a* 0,0,0, 0,0,$\frac{1}{2}$; 2*b* 0,0,$\frac{1}{4}$, 0,0,$\frac{3}{4}$; 2*c* $\frac{1}{3},\frac{2}{3},\frac{1}{4}$, $\frac{2}{3},\frac{1}{3},\frac{3}{4}$; 2*d* $\frac{2}{3},\frac{1}{3},\frac{1}{4}$, $\frac{1}{3},\frac{2}{3},\frac{3}{4}$; 4*f* $\frac{1}{3},\frac{2}{3},z$, $\frac{1}{3},\frac{2}{3},\frac{1}{2}-z$; $\frac{2}{3},\frac{1}{3},z+\frac{1}{2}$, $\frac{2}{3},\frac{1}{3},\bar{z}$.

III | $\sim 1105 - \sim 1360$ K | $P6_3/mcm$ (193) | $Z = 6$ | nonpolar, paramagnetic | unit-cell volume matches that of phases IV or V.

IV | 75–1105 K | $P6_3cm$ (185) | $Z = 6$ | ferroelectric, paramagnetic | 2 polar variants.

V | $\lesssim$ 75 K | *e.g.* $P6_3'c'm$ (185) |[2] $Z = 6$ | ferroelectric, antiferromagnetic | 2 polar variants.

The transformation between paramagnetic $YMnO_3$ phase IV and antiferromagnetic phase V at $T_N \simeq 80$ K, see §1, is clearly a phase transition with magnetic ordering for which the Shubnikov/magnetic space group (Koptsik, 1963; Litvin, 2001, 2008*a*,*b*) has still to be reported. Lee *et al.* (2008) give lattice constants $a = 6.12049$ (7), $c = 11.40756$ (2) Å at 10 K (see ambient values in Table 1).

The proposal that the transition between phases IV ↔ III in ferroelectric $YMnO_3$ is *ca* 935 K, as noted in §1, remained controversial until the unambiguous determination by Nénert *et al.* (2007) that $T_C \simeq 1105$ K between polar $P6_3cm$ and centrosymmetric $P6_3/mcm$. The ~ 1275 K temperature reported by Łukaszewicz & Karut-Kalicińska (1974) for the phase III ↔ II transition is identifiable with that given by Lonkai *et al.* (2004) as 1433 (27) K and by Nénert *et al.* (2007) as 1350 K, see also §5.

2.2. Phase transition order in hexagonal $YMnO_3$

Two entropy anomalies were observed by Nénert *et al.* (2007) in $YMnO_3$ using differential thermal analysis, the smaller at $T_{IV-III} \simeq 1100$ K, the larger at $T_{III-II} \simeq 1350$ K. Both are indicative of first-order phase transitions (FOPTs), although the entropy change was reported at neither.[3] Their dilatometric analysis, however, was suggestive of second order. Landau–Lifshitz criteria had previously led Nénert *et al.* (2005) to characterize the transition at T_{IV-III} as likely to be continuous, that at T_{III-II} a FOPT, *cf.* §4.2. The wide variation reported in the literature for the magnitudes of T_{IV-III} and T_{III-II} is most likely indicative of impurities, defects and/or disorder in the samples used, but such identification requires further study. The abrupt magnetic entropy and heat-capacity changes at $T_{V-IV} \simeq 75$ K reported by Lee *et al.* (2008), *cf.* §1, are strongly suggestive of a FOPT and in sharp contrast with the gradual transitions observed at T_{IV-III} or T_{III-II}.

3. Coordinate analysis of each phase in the $YMnO_3$ structure[4]

Atomic coordinate analysis allows any well determined phase to be investigated in order to reveal the atomic displacements required for a possible transition to another phase of higher but related symmetry. The method requires all differences between the atomic coordinates derived for the higher-symmetry structure and those corresponding in the original structure determination to be less than about $3u_{eq}$ at the transition temperature. The results of such analyses for phases I–IV of $YMnO_3$, based on van Aken *et al.*'s (2001) experimental coordinates measured at ambient temperature, are presented in Tables 1–4.

The structure of ferroelectric phase IV contains sheets of slightly tilted trigonal bipyramidal MnO_5 ions separated by sheets of independent pairs of pentagonal bipyramidal YO_7 ions, represented in Fig. 1 (Dowty, 2004) by large spheres. The Curie temperature T_C may be derived from the maximum Y^{+3} cation displacement by

$$T_C = (\kappa/2k)(\Delta z_i)^2 \text{ K}, \quad (1)$$

in which the force constant $\kappa = 5.52\,(25) \times 10^4$ kPa and the Boltzmann constant $k = 1.380658\,(12) \times 10^{-23}$ J K^{-1}; thus

[2] Or $P6_3cm1'$, $P6_3'cm'$ or $P6_3c'm'$, unless the antiferromagnetic unit cell undergoes an integral length or further symmetry change at T_N; experimental measurement is required for magnetic space-group determination, see Litvin (2008*b*), pp. 3656–3666.

[3] A FOPT is characterized by exhibiting a finite latent heat or entropy discontinuity.

[4] Except in the structurally undetermined phase V.

Table 3
Aken *et al.*'s (2001) transformed atomic coordinates for $YMnO_3$ in phases III and II, oriented to match the phase II orientation at 1275 K [Łukaszewicz & Karut-Kalicińska, 1974, estimate $a_I = a_{III}/(3)^{1/2} \simeq 3.61$ Å 'above 1273 K'], see values in Tables 1 and 2.

Ambient temperature lattice constants for phases II and I taken as $a_I = a_{III}/(3)^{1/2} \simeq 3.5442$, $c \simeq 11.40$ Å; $z^* = z + 0.03817$.

	Wyckoff position								Δx_{III-II}	Δy_{III-II}	Δz_{III-II}	$\Delta\xi_{III-II}$
	$P6_3/mcm$	$P6_3/mmc$†	x_{III}	y_{III}	z_{III}	x_{II}	y_{II}	z_{II}	(Å)	(Å)	(Å)	(Å)
Phase III → II‡												
Y1,Y2	2*b*	2*a*	0	0	$\frac{1}{2}$	0	0	$\frac{1}{2}$	0	0	0.0	0.0
Mn	4*c*	2*d*	$\frac{2}{3}$	$\frac{1}{3}$	$\frac{1}{4}$	$\frac{2}{3}$	$\frac{1}{3}$	$\frac{1}{4}$	0	0	0.0	0.0
O1,O2	4*d*	4*f*	$\frac{1}{3}$	$\frac{2}{3}$	0	$\frac{1}{3}$	$\frac{2}{3}$	0.087	0	0	0.99	0.99
O3,O4	2*a*	2*b*	0	0	$\frac{1}{4}$	0	0	$\frac{1}{4}$	0	0	0	0

† Wyckoff positions in $P6_3/mcm$: see Table 1; in $P6_3/mmc$: see Table 2. ‡ With only one variable coordinate in phase II, Łukaszewicz & Karut-Kalicińska's (1974) estimated value z_I(O2) = 0.085 is notably within ∼ 0.025 Å of that derived by coordinate analysis for z_I(O1,O2).

Table 4
Aken *et al.*'s (2001) transformed atomic coordinates for $YMnO_3$ in phases II and I, oriented to match those at 1275 K used by Łukaszewicz & Karut-Kalicińska (1974), see values in Table 3.

Ambient temperature lattice constants for phases II and I taken as $a_I \simeq 3.5442$, $c_I = c_{II}/2 \simeq 5.70$ Å; $z^* = z + 0.03817$.

	Wyckoff position								Δx_{II-I}	Δy_{II-I}	Δz_{II-I}	$\Delta\xi_{II-I}$
	$P6_3/mmc$	$P6/mmm$†	x_{II}	y_{II}	z_{II}‡	x_I	y_I	z_I	(Å)	(Å)	(Å)	(Å)
Phase II → I												
Y1,Y2	2*a*	1*a*	0	0	0	0	0	0	0	0	0.0	0.0
Mn	2*d*	2*d*	$\frac{2}{3}$	$\frac{1}{3}$	$\frac{1}{4}$	$\frac{2}{3}$	$\frac{1}{3}$	$\frac{1}{2}$	0	0	0.0	0.0
O1,O2	4*f*	2*c*	$\frac{1}{3}$	$\frac{2}{3}$	0.087	$\frac{1}{3}$	$\frac{2}{3}$	0	0	0	0.99	0.99
O3,O4	2*b*	1*b*	0	0	$\frac{1}{4}$	0	0	$\frac{1}{2}$	0	0	0	0

† Wyckoff positions in $P6/mmm$: 1*a* 0,0,0; 1*b* 0,0,$\frac{1}{2}$; 2*c* $\frac{1}{3},\frac{2}{3}$,0; $\frac{2}{3},\frac{1}{3}$,0; 2*d* $\frac{1}{3},\frac{2}{3},\frac{1}{2}$; $\frac{2}{3},\frac{1}{3},\frac{1}{2}$; 2*e* 0,0,*z*; 0,0,$\bar{z}$; 3*f* $\frac{1}{2}$,0,0; $\frac{1}{2},\frac{1}{2}$,0; 3*g* $\frac{1}{2}$,0,$\frac{1}{2}$; 0,$\frac{1}{2},\frac{1}{2}$; $\frac{1}{2},\frac{1}{2},\frac{1}{2}$; 4*h* $\frac{1}{3},\frac{2}{3}$,*z*; $\frac{2}{3},\frac{1}{3}$,*z*; $\frac{1}{3},\frac{2}{3}$,$\bar{z}$; $\frac{2}{3},\frac{1}{3},\bar{z}$. ‡ It is noted that $c_I = c_{II}/2$.

$\kappa/2k = 2.00\ (9) \times 10^4$ K Å^{-2}, where Δz_i is the largest *i*-cationic displacement at T_C between its measured location and that along the polar axis at which the spontaneous polarization P_S would be zero (Abrahams *et al.*, 1968).

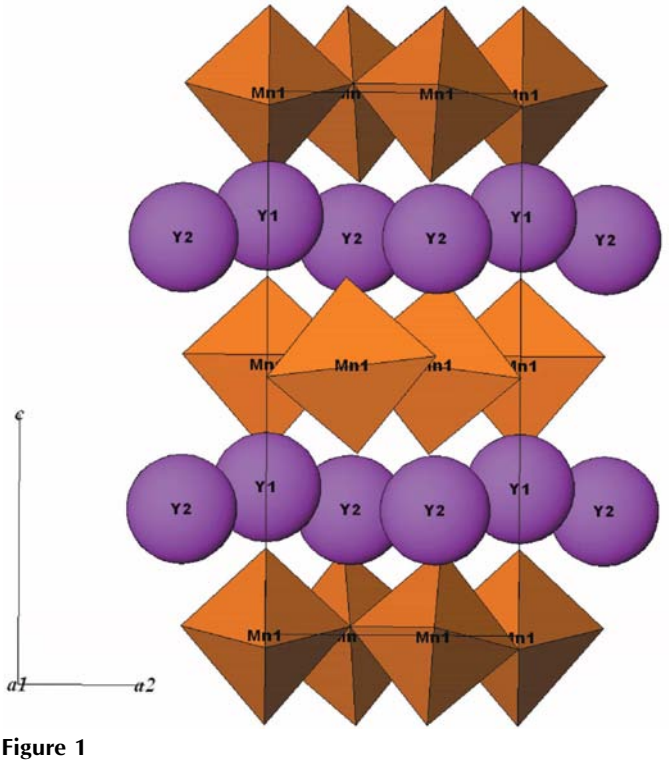

Figure 1
Unit-cell contents of $YMnO_3$ phase IV along the a_1 axis, see Table 1, based on the atomic coordinates of Aken *et al.* (2001).

3.1. Transition between phases IV and III in $YMnO_3$

The maximum displacements in $YMnO_3$ at the transition from ferroelectric phase IV to nonpolar phase III are Δz_{IV-III}(Y1) = 0.270 and Δz_{IV-III}(Y2) = 0.195 Å, see Table 1. Such large differences between the displacement of cations predicted to become equivalent in phase III, with unit-cell volume 1/3 that at ambient temperature, are assumed to result from the wide spread between the experimental temperature and that predicted for the transition to phase III (T_{IV-III}). The resulting inequality between Δz_{IV-III}(Y1) and Δz_{IV-III}(Y2) is expected to decrease with rising temperature, *i.e.* as ($T_{IV-III} - T_{exp}$) approaches zero, z_{III} is expected to approach $z' = (z'_{IV} + z'_{III})/2$. The resulting $\langle\Delta z(Y)\rangle$ = 0.232 Å corresponds to T_{IV-III} = 1076 K, notably close to the experimental T_C = 1105 K.

3.2. Transition between phases III and II in $YMnO_3$

The possibility that the transition from phase IV to phase III in $YMnO_3$ is followed by a further transition from phase III to phase II *versus* the alternative of a transition directly from phase IV to phase II at higher temperature is readily evaluated by coordinate analysis, see Tables 1 and 2. Identical displacements by Y1 and Y2 at either transition, with both Y atoms occupying comparable special positions in $P6_3/mcm$ and in $P6_3/mmc$, favor neither space group. The Mn atom, within

~ 0.01 Å of either the special 6*g* position in phase III or the 2*d* position in the smaller unit cell of phase II, requires a negligibly small displacement for such a transition to either alternative phase. The principal difference between Tables 1 and 2 is thus associated with the magnitude of corresponding Δy(O) atomic displacements; the significantly smaller $\Delta\xi$(O1/O2) values in Table 1 favor the observed transition from space group $P6_3cm$ to intermediate $P6_3/mcm$ thermodynamically over that required in Table 2 to the higher-temperature $P6_3/mmc$ phase. The consequent atomic arrangement in phases III and II is thus very similar, see Figs. 2 and 3, with the O—Mn—O bipyramidal ion axis parallel to the polar axis in both, in contrast to the arrangement in phase IV. The primary change in the latter on heating through T_C is loss of the bipyramidal axis tilt in phase III. The structural similarities noted may be seen in Figs. 3 and 4, the views in the latter complementing those in Figs. 1 and 2 by provision of the third dimension.

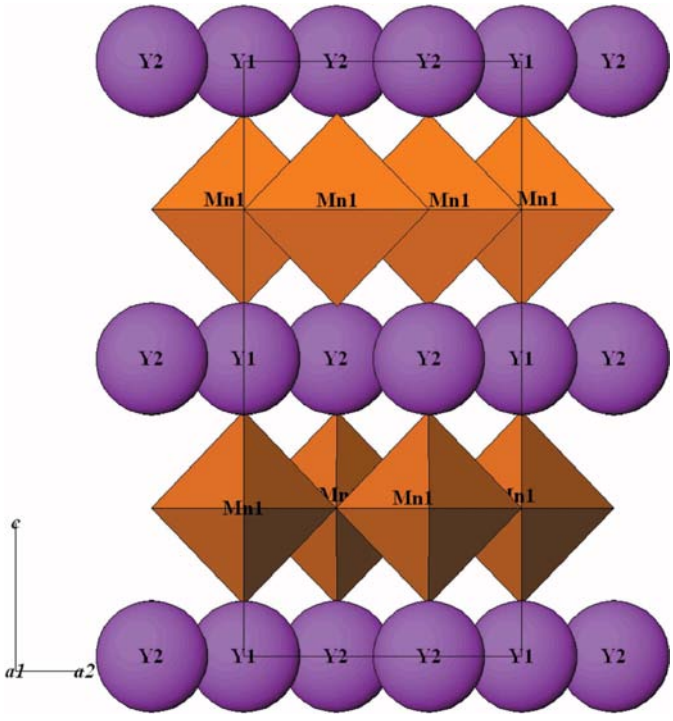

Figure 2
Unit-cell contents of $YMnO_3$ in phase III along the a_1 axis, see Table 2.

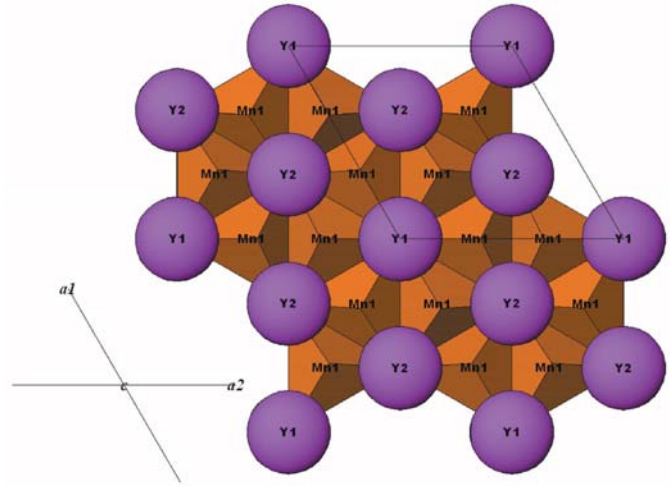

Figure 3
Four unit cells of $YMnO_3$ in phase II along the *c* axis, see Table 3.

3.3. Transition between phases II and I in $YMnO_3$

If the ~ 0.08 Å difference between $\Delta(Y1)z_{IV-III}$ and $\Delta(Y2)z_{IV-III}$ in Table 1 is an indicator of a previously unsuspected higher-temperature phase transition in $YMnO_3$, *cf.* §4, then the latter may be predicted as from space group $P6_3/mmc$ in phase II to aristotype phase I with space group $P6/mmm$, the latter supergroup to $P6_3/mmc$. The unit-cell *c*-axis length in phase I is necessarily reduced by a factor of 2 from that in phase II, see *International Tables for Crystallography* (1987, Vol. A), with the *a* and *b* axes in phase I reduced by the same $3^{1/2}$ factor as in phase II from that in phases III or polar IV, see Fig. 4. Landau theory allows the proposed phase II $\leftrightarrow$ I transition at $T \gtrsim 1600$ K to be continuous; a displacement of ~ 0.99 Å by the O1/O2 atom in a fourfold Wyckoff location is hence the only requirement for such a transition, see Table 4, assuming the crystal is thermally stable at T_{II-I}. Although an O atom displacement of 0.99 Å magnitude might be questionable at a transition temperature closer to ambience, this value is identical to that determined structurally by Łukaszewicz & Karut-Kalicińska (1974) in the III $\leftrightarrow$ II phase transition. The resulting $d_{Y-O} = 2.046$ Å bond lengths in phase I, uncorrected either for axial or bond-length thermal expansion, are comparable to those in phase IV; the calculated d_{Mn-O} lengths, however, are identical to those of d_{Y-O} although expected to be ~ 0.4–0.5 Å shorter. Experimental determi-

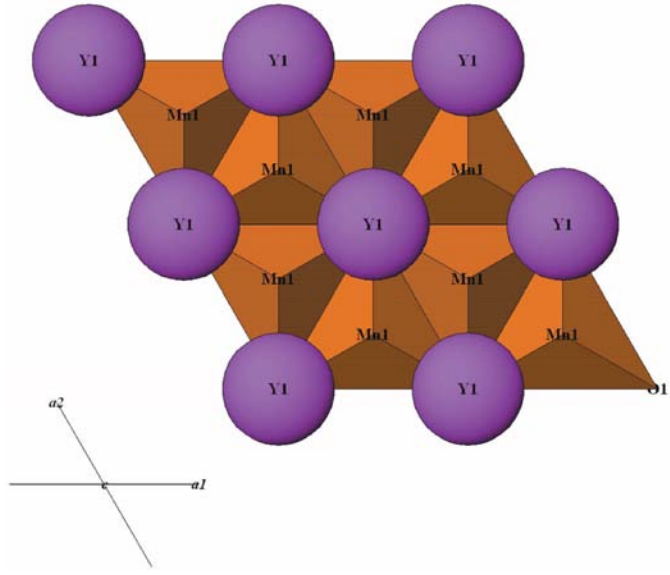

Figure 4
Four unit cells of $YMnO_3$ in phase I along the *c* axis, see Table 4.

nation of the postulated structure in phase I, in addition to redetermination of the structure in phase II, is necessary for confirmation of the predictions above.

The possibility that hexagonal $YMnO_3$ might also be subject to structural disorder comparable to that in $BaTiO_3$ or to impurities or defects, see §5, does not yet appear to have been investigated. If such effects are detected in $YMnO_3$, consideration of their possible interactions with the ionic displacements at each transition would become necessary.

4. Multiferroic multiphase tetragonal $BaTiO_3$[5]

More than 80% of all crystals investigated are reported to undergo a single phase transition (*cf.* Tomaszewski, 1992), with relatively few exhibiting three or more phase transitions as in $YMnO_3$ and even fewer that are ferroelectric with all phases fully investigated structurally. A prominent multiphase ferroelectric material meeting the latter conditions is $BaTiO_3$, the third ferroelectric discovered [by von Hippel *et al.* (1946) and, independently, Wul & Vereschagen (1946)].[6] The properties of multiferroic $BaTiO_3$ have been the subject of numerous investigations,[7] several of which provide information pertinent to the properties of $YMnO_3$, see *e.g.* §4.2; a summary of the more relevant results follows.

Landau theory allows the phase I ↔ II transition between the space groups $Pm\overline{3}m$ and $P4mm$ in $BaTiO_3$ to be continuous, since phase II is a subgroup of phase I; experimentally, this transition strongly exhibits first-order characteristics, see §4.2. Neither the phase II ↔ III transition between space groups $P4mm$ and $Amm2$, nor the phase III ↔ IV transition between space groups $Amm2$ and $R3m$, are supergroup–subgroup related hence, as Howard & Stokes (2005) observe on the basis of Landau theory: 'a transition that does not correspond to a group–subgroup pair *cannot* be continuous and, should such a phase transition occur, *must* be of first order'.[8] This aspect of the phase transitions in $BaTiO_3$ is comparable to that in $YMnO_3$, albeit at much lower temperatures, see also §2.2 and Satoh *et al.* (1998).

The unit cells both of cubic aristotype phase I and tetragonal phase II in $BaTiO_3$ have $a \simeq c \simeq 4$ Å,[9] but the orthorhombic phase III unit-cell volume is close to double that in phases I and II due to a 45° rotation about the a axis resulting in $b \simeq c \simeq 4(2)^{1/2}$ Å. The rhombohedral phase IV unit-cell volume, with $a \simeq 4$ Å and $\alpha \simeq 89.4°$, approaches that of phases I and II. All calculations in Tables S1–S29,[10] presenting the magnitudes of Δz and $\Delta\xi$ as defined in Table 1 and derived at each temperature measured, make due allowance for the phase transformations at $T_{II-I}^{exp} \simeq 393$, $T_{III-II}^{exp} \simeq 278$ and $T_{IV-III}^{exp} \simeq 183$ K, see also §4.2.

Numerous structural studies of the $BaTiO_3$ phase sequence have been reported as a function of increasing temperature. Among them, the results of Kwei *et al.* (1993), based on structural refinement using powder diffraction data measured at five or more temperatures within each phase,[11] are noteworthy in showing that all relative atomic positions remain nearly constant throughout each phase, a conclusion supported by the thermally independent Δz_i value implicit in (1) and taken as applicable to $YMnO_3$. Darlington *et al.*'s (1994) thermally dependent structural measurements on $BaTiO_3$ are similarly suggestive of general Δz_i magnitude constancy throughout each phase,[12] but the graphical presentation hinders quantitative use in the present study.

$BaTiO_3$ in the space group $Pm\overline{3}m$ exhibits six structurally identical Ti—O bond lengths of 2.0029 (8) Å, changing abruptly at the phase transition to $P4mm$ with one d_{Ti-O} of 1.87 (2) Å, another of 1.877 (9) Å and four of 2.004 (1) Å (Buttner & Maslen, 1992), consistent with a FOPT. Kwei *et al.* (1993) report d_{Ti-O} = 1.838 (9), 2.198 (9) and four of 2.002 (9) Å. At the transition to $Amm2$, the latter give two d_{Ti-O} each of 1.875 (1), 1.996 (2) and 2.146 (2) Å and, following the transition to space group $R3m$, three of 1.878 (2) and three of 2.134 (2) Å.

4.1. Predicted *versus* measured atomic displacements at the $BaTiO_3$ phase transitions

The $BaTiO_3$ atomic displacement $\Delta Ti(z)_{II-I}$ corresponding to the experimental Curie temperature T_{II-I}^{exp} = 393 K for the phase II ↔ I transition is 0.140 Å, based on (1). Kwei *et al.*'s (1993) mean value over the 350–280 K range is $\Delta Ti(\langle z\rangle)_{II-I}$ = 0.099 (3) Å,[13] that over the 270–190 K range is $\Delta Ti(\langle z\rangle)_{III-II}$ = 0.102 (12) Å and over the 180–15 K range is $\Delta Ti(\langle z\rangle)_{IV-III}$ = 0.120 (12) Å, see Tables S1–S19. Five additional studies of phase II by Kim *et al.* (2000), Aoyagi *et al.* (2002), Buttner & Maslen (1992), Jiang *et al.* (1988) and Harada *et al.* (1970), see Tables S20–S24, average to $\Delta Ti(z)_{II-I}$ = 0.097 (20) Å, in fair agreement with Kwei *et al.* (1993).

The phase III ↔ II transition temperature T_{III-II}^{exp} = 278 K corresponds to $\Delta Ti(z)_{III-II}$ = 0.118 Å by (1), with Kwei *et al.*'s (1993) coordinates in Tables S6–S10 averaging to 0.102 (12) Å.

[5] A second polymorphic form of $BaTiO_3$ with hexagonal symmetry and space group $P6/mmc$ at ambience, with a transition at ∼ 70 K to the space group $C222_1$, forms another phase below ∼ 7 K that probably has the space group $P2_1$ (Yamamoto *et al.*, 1988), but is not considered further here.

[6] The property of ferroelectricity, first discovered in Rochelle salt by Valasek (1921), then in KH_2PO_4 by Busch & Scherrer (1935), remained an interesting curiousity until $BaTiO_3$ was found during WWII to be ferroelectric, with useful physical properties. Early reports on $BaTiO_3$ were classified, hence publication was deferred.

[7] Including the ferroelastic properties of ferroelectric phase II, see *e.g.* Hlinka (2007).

[8] Emphasis added.

[9] Recent claims by Yoshimura *et al.* (2007) that monoclinic and tetragonal phases of $BaTiO_3$ coexist below T_{II-I}^{exp} have been shown by Keeble & Thomas (2009) to be nonconfirmable.

[10] Supplementary data for this paper, including Tables S1–S29 of the thermally dependent $BaTiO_3$ atomic coordinates in space groups $P4mm$, $Amm2$ and $R3m$, their derivative symmetry and resulting atomic displacements over the range 350 to 15 K and to 3.2 GPa, are available from the IUCr electronic archives (Reference: BK5086). Services for accessing these data are described at the back of the journal.

[11] Kwei *et al.* (1993) consistently refer to the space group of ferroelectric tetragonal $BaTiO_3$ as (nonpolar) $P4/mmm$ but present results in a form consistent with Ti and both O atoms occupying locations corresponding to 1*b* and 2*c* in polar $P4mm$, the well substantiated polar space group.

[12] The authors note both O(z) magnitudes 'are almost exactly the same over the whole temperature range studied'.

[13] The uncertainty stated is the standard deviation of the average displacement.

The remaining study of phase III at ambient pressure, see Shirane *et al.* (1957) in Table S25, gives $\Delta\mathrm{Ti}(z)_{\mathrm{III-II}} = 0.12$ Å.

The phase IV $\leftrightarrow$ III transition temperature $T_{\mathrm{IV-III}}^{\mathrm{exp}} = 183$ K corresponds to $\Delta\mathrm{Ti}(z)_{\mathrm{IV-III}} = 0.096$ Å by (1), while averaging Kwei *et al.*'s (1993) values in Tables S11–S19 gives 0.120 (16) Å. Hewat's (1974) and Schildkamp & Fischer's (1981) coordinates in Tables S26–S27 result in 0.134 and 0.116 Å, respectively.

The average experimental magnitude of $\Delta\mathrm{Ti}(z)$ in $BaTiO_3$ at each of the successive transitions from the lowest-temperature ferroelectric to the aristotype phase is hence either (*a*) close to a constant 0.107 Å at each of the three phase transitions or (*b*) increases ~ 0.020 Å between the lowest and highest phase transitions. The experimental $\Delta\mathrm{Ti}(z)$ uncertainty of ~ 0.02 Å in the studies available is insufficient to resolve the choice; notably, however, the change in $|\Delta\mathrm{Ti}(z)|$ over the phase succession is clearly close to negligible.

This result suggests the possibility that if a material undergoes more than a single phase transition, of which one is ferroelectric, then all other ferrroelectric phases present will exhibit a $\Delta(z)$ value identical to that at the phase transition with the highest T_{C} value. If only one ferroelectric phase is formed, as in $YMnO_3$, then its major $\Delta(z)$ value determines the highest phase-transition temperature, as assumed in §3.3.

4.2. Thermal dependence of physical properties and phase transition order in $BaTiO_3$

Many properties of tetragonal $BaTiO_3$ such as the lattice constants (Clarke, 1976), the dielectric constant, spontaneous polarization, coercive field, birefringence, specific heat, thermal expansion and others (see *e.g.* Hellwege, 1981) have thermal dependences that exhibit sharp discontinuities, indicative of first order, at each phase transition. The λ-point heat capacity anomaly at the 393 K phase I $\leftrightarrow$ II transition with entropy change 0.53 J mol^{-1} K^{-1}, for example, is fully characteristic of a FOPT between space groups $Pm\overline{3}m$ and $P4mm$, although its supergroup–subgroup relation allows a continuous transition, *cf.* §4, also Strukov *et al.* (2004).[14]

5. Influence of impurities, defects and structural disorder on phase transitions

The influence of impurities and defects on ferroelectric and other phase transitions is often consequential and their study has led to a growing literature, *e.g.* Lebedev *et al.* (1997). The wide variation reported in $YMnO_3$ phase-transition temperatures may be related to the presence of impurities or defects, but such an origin has yet to be reported. The X-ray diffuse scattering discernable in all four $BaTiO_3$ phases was proposed by Comès *et al.* (1970) as being due to the linearly disordered central Ti atom and as phase-specific. Numerous experimental investigations including Verble *et al.*'s (2005) Raman scattering measurements together with Zhong *et al.*'s (1994) first-principles calculations and Pirc & Blinc's (2004) dynamic response derivation have amply confirmed the presense of order–disorder scattering components in $BaTiO_3$. A detailed investigation of this contribution, including a correction for any influence on the atomic coordinates and phase transitions in addition to the complementary structural and displacive aspects considered above, would be most appropriate.

6. Structural pressure-dependence in ferroelectric phases

Bos *et al.* (2001) report orthorhombic $YMnO_3$ forms under 15 kbar hydrostatic pressure, the hexagonal phase at lower pressures, while Jaouen *et al.* (2007) note that the application of 13 GPa to $PbTiO_3$ (space group $P4mm$) reduces the equilibrium Ti-atom displacement to 0.090 (15) Å. The structural pressure-dependence of $BaTiO_3$ in phase II was determined by Hayward *et al.* (2005) at 0.2 GPa and 298 K and at 3.2 GPa and 213 K, also in phase III at 3.2 GPa and 165 K, see Tables S28–S30; the former resulted in $\Delta\mathrm{Ti}(z)_{\mathrm{I-II}} \simeq 0.07$ Å, corresponding to $T_{\mathrm{I-II}}^{\mathrm{calc}} \simeq 100$ K by use of (1), hence indicative of a strongly depressed Curie temperature. The structure in phase III at 213 K returned to cubic symmetry under 3.2 GPa as $\Delta\mathrm{Ti}(z)_{\mathrm{III}} \rightarrow 0$.

The orthorhombic $BaTiO_3$ phase at 165 K (18 K below the phase III/IV boundary at ambient pressure) closely approaches cubic symmetry under a pressure of 3.2 GPa. The transition temperature between paraelectric and ferroelectric phases is hence reduced strongly by the application of hydrostatic pressure, with full suppression of T_{C} at higher pressures. An approximately linear relationship between spontaneous strain e_s and the quantity Δz_{Ti}^2, a relationship comparable with (1), was recognized by Hayward *et al.* (2005).

7. Summary

The four known phases of $YMnO_3$, one antiferromagnetic, one ferroelectric and two nonpolar, have been characterized by cooordinate analysis. A new aristotype nonpolar phase I is predicted to form at $T \gtrsim 1600$ K. Experimental and predicted atomic displacement and T_{C} values agree within their uncertainties at each phase transition. Both the I $\leftrightarrow$ II and III $\leftrightarrow$ IV phase transitions, each between a supergroup and its subgroup, are allowed by Landau theory to be continuous. Although phase II is a maximal nonisomorphic subgroup of phase III, this transition fails to satisfy a supergroup–subgroup relationship since the order–parameter expansion contains odd-order terms,[15] hence the II $\leftrightarrow$ III phase transition must be first order. Magnetic symmetry and structural information on phase V has yet to be reported but, experimentally, the IV $\leftrightarrow$ V phase transition exhibits first-order characteristics as do the three other phase transitions in $YMnO_3$. The same observation and conclusion apply to all three phase transitions in $BaTiO_3$, although the phase I $\leftrightarrow$ II transition at 393 K is allowed by Landau theory to be continuous. A generalization

[14] The authors note the latent heat is dependent both on particle size and supporting film thickness.

[15] Indebtness is acknowledged to an anonymous referee for this statement.

concerning multiphase transition materials, of which one at least is ferroelectric, is proposed.

Professors Th. Hahn, J. Kobayashi, P. Photinos, H. Satoh and H. T. Stokes are warmly thanked for most helpful comments, as is a most perceptive anonymous referee for clarifying observations, see footnote 15. Support of this research by the National Science Foundation (DMR-0137323) is gratefully acknowledged.

References

Abrahams, S. C. (2001). *Acta Cryst.* B**57**, 485–490.
Abrahams, S. C., Kurtz, S. K. & Jamieson, P. B. (1968). *Phys. Rev.* **172**, 551–553.
Aken, B. B. van, Meetsma, A. & Palstra, T. T. M. (2001). *Acta Cryst.* C**57**, 230–232.
Aken, B. B. van, Palstra, T. T. M., Filippetti, A. & Spaldin, N. A. (2004). *Nature Mater.* **3**, 164–170.
Aoyagi, S., Kuroiwa, Y., Sawada, A., Yamashita, I. & Atake, T. (2002). *J. Phys. Soc. Jpn*, **71**, 1218–1221.
Bos, J.-W., van Aken, B. B. & Palstra, T. T. M. (2001). *Chem. Mater.* **13**, 4804–4807.
Busch, G. & Scherrer, P. (1935). *Naturwissenschaften*, **43**, 737.
Buttner, R. H. & Maslen, E. N. (1992). *Acta Cryst.* B**48**, 764–769.
Clarke, R. (1976). *J. Appl. Cryst.* **9**, 335–338.
Comès, R., Lambert, M. & Guinier, A. (1970). *Acta Cryst.* A**26**, 244–254.
Darlington, C. N. W., David, W. I. F. & Knight, K. S. (1994). *Phase Transitions*, **48**, 217–236.
Dowty, E. (2004). *ATOMS*, Version 6.2. Shape Software, Kingsport, Tennessee, USA, http://www.shapesoftware.com.
Fennie, C. J. & Rabe, K. M. (2008). http://arxiv.org/ftp/cond-mat/papers/0504/0504546.pdf.
Fujimura, N., Shigemitsu, N., Takahashi, T., Ashida, A., Yoshimura, T., Fukumura, H. & Harima, H. (2007). *Philos. Mag. Lett.* **87**, 193–201.
Harada, J., Pedersen, T. & Barnea, Z. (1970). *Acta Cryst.* A**26**, 336–344.
Hayward, S. A., Redfern, S. A. T., Stone, H. J., Tucker, M. G., Whittle, K. R. & Marshall, W. G. (2005). *Z. Kristallogr.* **220**, 735–739.
Hellwege, K.-H. (1981). Editor. *Landolt–Börnstein Numerical Data and Functional Relationships in Science and Technology*, New Series, Vol. 16(a). Berlin: Springer-Verlag.
Hewat, A. W. (1974). *Ferroelectrics*, **6**, 215–218.
Hippel, A. von, Breckenridge, R. G., Chesley, F. G. & Tisza, L. (1946). *Ind. Eng. Chem.* **38**, 1097–1109, and unpublished earlier ONR reports.
Hlinka, J. (2007). *Ferroelectrics*, **349**, 49–54.
Howard, C. J. & Stokes, H. T. (2005). *Acta Cryst.* A**61**, 93–111.
Huang, Z. J., Cao, Y., Sun, Y. Y., Xue, Y. Y. & Chu, C. W. (1997). *Phys. Rev. B*, **56**, 2623–2626.
Ismailzade, I. G. & Kizhaev, S. A. (1965). *Sov. Phys. Solid State*, **7**, 236–238.
Janoschek, M., Rössli, B., Keller, L., Gvasaliya, K., Conder, K. & Pomjakushina, E. (2005). *J. Phys. Condens. Mater.* **17**, L425–L430.
Jaouen, N., Dhaussy, A. C., Itié, J. P., Rogalev, A., Marinel, S. & Joly, Y. (2007). *Phys. Rev. B*, **75**, 224115.
Jeong, I.-K., Hur, N. & Proffen, Th. (2007). *J. Appl. Cryst.* **40**, 730–734.
Jiang, Y.-J., Li, J.-Z. & Zeng, L. (1988). *Acta Phys. Sin.* **37**, 680–682.
Katsufuji, T., Masaki, M., Machida, A., Morimoto, M., Kato, K., Nishibori, E., Takata, M., Sakata, M., Ohoyama, K., Kitazawa, K. & Takagi, H. (2002). *Phys. Rev. B*, **66**, 134434, 1–8.
Keeble, D. S. & Thomas, P. A. (2009). *J. Appl. Cryst.* **42**, 480–484.
Kim, S. E., Lee, S. H., Kim, T. H., Zyung, T., Jeong, Y. H. & Jang, M. S. (2000). *Cryst. Res. Tech.* **35**, 19–27.
Koptsik, V. A. (1963). *Shubnikov Groups.* Moscow: Izd. MGU.
Kwei, G. H., Lawson, A. C., Billinge, S. J. L. & Cheong, S.-W. (1993). *J. Phys. Chem.* **97**, 2368–2377.
Lancaster, T., Blundell, S. J., Andreica, D., Janoschek, M., Roessli, B., Gvasaliya, S. N., Conder, K., Pomjakushina, E., Brooks, M. L., Baker, P. J., Prabhakaran, D., Hayes, W. & Pratt, F. L. (2007). *Phys. Rev. Lett.* **98**, 197203.
Lebedev, A. I., Sluchinskaya, I. A., Demin, V. N. & Munro, I. H. (1997). *Phase Transitions*, **60**, 67–77.
Lee, S., Pirogov, A., Kang, M., Kwang-Hyun, J., Yonemura, M., Kamiyama, T., Cheong, S.-W., Gozzo, F., Shin, N., Kimura, H., Noda, Y. & Park, J.-G. (2008). *Nature*, **451**, 805–809.
Litvin, D. B. (2001). *Acta Cryst.* A**57**, 729–730.
Litvin, D. B. (2008*a*). *Acta Cryst.* A**64**, 419–424.
Litvin, D. B. (2008*b*). *Magnetic Space Groups Book*, pp. 3656–3666. http://www.bk.psu.edu/faculty/Litvin/V1.3_Magnetic_Space_Groups_Book.pdf.
Lonkai, T., Tomuta, D. G., Amann, U., Ihringer, J., Hendrikx, R. W. A., Többens, D. M. & Mydosh, J. A. (2004). *Phys. Rev. B*, **69**, 134108, 1–10.
Łukaszewicz, K. & Karut-Kalicińska, J. (1974). *Ferroelectrics*, **7**, 81–82.
Nénert, G., Pollet, M., Marinel, S., Blake, G. R., Meetsma, A. & Palstra, T. T. M. (2007). *J. Phys. Condens. Matter*, **19**, 466212, 1–8.
Nénert, G., Ren, Y., Pollet, M., Hauback, B., de Moreira, I. P. R., Marinel, S., Stokes, H. T. & Palstra, T. T. M. (2006). *Acta Cryst.* A**62**, s121.
Nénert, G., Yang, R., Stokes, H. T. & Palstra, T. T. M. (2005). http://arxiv.org/ftp/cond-mat/papers/0504/0504546.pdf.
Pirc, R. & Blinc, R. (2004). *Phys. Rev. B*, **70**, 134107.
Satoh, H., Iwasaki, J.-I., Kawase, K. & Karnegashira, N. (1998). *J. Alloys Compd*, **268**, 42–46.
Schildkamp, W. & Fischer, K. (1981). *Z. Kristallogr.* **155**, 217–226.
Shirane, G., Danner, H. R. & Pepinsky, R. (1957). *Phys. Rev.* **105**, 856–860.
Strukov, B. A., Davitadze, S. T., Shulman, S. G., Goltzman, B. V. & Lemanov, V. V. (2004). *Ferroelectrics*, **301**, 157–162.
Tolédano, J.-C., Glazer, A. M., Hahn, Th., Parthé, E., Roth, R. S., Berry, R. S., Metselaar, R. & Abrahams, S. C. (1998). *Acta Cryst.* A**54**, 1028–1033.
Tomaszewski, P. E. (1992). *Phase Transitions*, **38**, 127–220.
Valasek, J. (1921). *Phys. Rev.* **17**, 475–481.
Verble, J. L., Gallego-Lluesma, E. & Porto, S. P. S. (2005). *J. Raman Spectrosc.* pp. 7–9.
Wul, B. M. & Vereschagen, L. F. (1946). *C. R. Acad. Sci. URSS*, **48**, 634.
Yamamoto, T., Akishige, Y. & Sawaguchi, E. (1988). *J. Phys. Soc. Jpn*, **57**, 3665–3670.
Yoshimura, Y., Morioka, M., Kojima, A., Tokunaga, N., Koganezawa, T. & Tozaki, K. (2007). *Phys. Lett. A*, **367**, 394–401.
Zhong, W., Vanderbilt, D. & Rabe, K. M. (1994). *Phys. Rev. Lett.* **73**, 1861–1864.